THE JOURNAL OF BIOLOGICAL CHEMISTRY VOL. 286, NO. 5, pp. 3630–3644, February 4, 2011

Activation of Vinculin Induced by Cholinergic Stimulation Regulates Contraction of Tracheal Smooth Muscle Tissue*[S]

Received for publication, April 30, 2010, and in revised form, October 19, 2010 Published, JBC Papers in Press, November 11, 2010, DOI 10.1074/jbc.M110.139923

Youliang Huang, Wenwu Zhang, and Susan J. Gunst[1]

From the Department of Cellular & Integrative Physiology, Indiana University School of Medicine, Indianapolis, Indiana 46202

Vinculin localizes to membrane adhesion junctions where it links actin filaments to the extracellular matrix by binding to the integrin-binding protein talin at its head domain (Vh) and to actin filaments at its tail domain (Vt). Vinculin can assume an inactive (closed) conformation in which Vh and Vt bind to each other, masking the binding sites for actin and talin, and an active (open) conformation in which the binding sites for talin and actin are exposed. We hypothesized that the contractile activation of smooth muscle tissues might regulate the activation of vinculin and thereby contribute to the regulation of contractile tension. Stimulation of tracheal smooth muscle tissues with acetylcholine (ACh) induced the recruitment of vinculin to cell membrane and its interaction with talin and increased the phosphorylation of membrane-localized vinculin at the C-terminal Tyr-1065. Expression of recombinant vinculin head domain peptide (Vh) in smooth muscle tissues, but not the talin-binding deficient mutant head domain, VhA50I, inhibited the ACh-induced recruitment of endogenous vinculin to the membrane and the interaction of vinculin with talin and also inhibited vinculin phosphorylation. Expression of Vh peptide also inhibited ACh-induced smooth muscle contraction and inhibited ACh-induced actin polymerization; however, it did not affect myosin light chain phosphorylation, which is necessary for cross-bridge cycling. Inactivation of RhoA inhibited vinculin activation in response to ACh. We conclude that ACh stimulation regulates vinculin activation in tracheal smooth muscle via RhoA and that vinculin activation contributes to the regulation of active tension by facilitating connections between actin filaments and talin-integrin adhesion complexes and by mediating the initiation of actin polymerization.

Actin-activated cross-bridge cycling is widely accepted as the mechanism by which contractile stimuli induce shortening and tension development in both striated and smooth muscle tissues (1, 2). In smooth muscle tissues, phosphorylation of the 20-kDa light chain of myosin is well established as the primary mechanism for the regulation of cross-bridge activation in response to contractile stimuli (2). However, there is growing evidence that tension development in smooth muscle also depends on dynamic cytoskeletal processes outside of the actomyosin interaction (3, 4). In tracheal smooth muscle, contractile stimulation initiates an integrated array of cytoskeletal events that are orchestrated by macromolecular protein complexes at adhesion junctions where cytoskeletal proteins link actin filaments to the extracellular matrix. Pathways mediated by adhesion complex proteins collaborate with pathways initiated by G-protein-coupled receptors to initiate cytoskeletal processes that regulate both actin polymerization and the activation of actomyosin cross-bridge cycling. Evidence from studies of a variety of smooth muscle tissues indicates that processes of cytoskeletal remodeling and actin polymerization as well as cross-bridge cycling are both necessary for active tension development and that neither process can mediate tension development by itself (3, 5–12).

Vinculin is a multidomain protein that localizes to adhesion junctions where actin filaments are linked to the extracellular matrix. Vinculin binds to the integrin-binding proteins talin and α-actinin, as well as to filamentous actin (13–18). In model cell systems, vinculin is recruited to talin-integrin adhesion complexes during adhesion and migration, and vinculin recruitment correlates with strengthening of the force-bearing linkages to the extracellular matrix at these junctions (19–22). Vinculin and its closely related isoform, metavinculin, are well documented constituents of adhesion junctions in smooth muscle cells (SMCs)[2] and tissues (23–25). In tracheal smooth muscle, more vinculin localizes to the plasma membrane in cells stimulated with a contractile agonist than in unstimulated cells (26, 27).

The conformational state of the vinculin molecule can be reversibly regulated between an activated "open" state and an inactive "auto-inhibited" state (13, 14, 16, 17, 28–30). In the open state, the head domain of vinculin (Vh) can bind to talin and α-actinin, and the vinculin tail domain (Vt) can bind to actin filaments, thus supporting linkages between the actin cytoskeleton and integrin adhesion junctions (13, 17, 29, 31). In its auto-inhibited state, the head and tail regions of vinculin are tightly associated, allosterically blocking the interaction of vinculin with talin and actin filaments and preventing the formation of vinculin-talin-integrin complexes (29).

* This work was supported, in whole or in part, by National Institutes of Health Grants HL29289 and HL074099. This work was also supported by an American Heart Association post-doctoral fellowship (to Y. H.) and an American Lung Association post-doctoral fellowship (to W. Z.).

[S] The on-line version of this article (available at http://www.jbc.org) contains supplemental movie S1 and Figs. S1–S3.

[1] To whom correspondence should be addressed: Dept. of Cellular and Integrative Physiology, Indiana University School of Medicine, 635 Barnhill Dr., Indianapolis, IN 46202. Tel.: 317-274-4108; Fax: 317-274-3318; E-mail: sgunst@iupui.edu.

[2] The abbreviations used are: SMC, smooth muscle cell; Vh, vinculin head domain; Vt, vinculin tail domain; N-WASp, neuronal Wiskott-Aldrich Syndrome protein; PLA, proximity ligation assay; TES, 2-{[2-hydroxy-1,1-bis(hydroxymethyl)ethyl]amino}ethanesulfonic acid; MLC, myosin light chain; ACh, acetylcholine; Arp, actin-related protein; US, unstimulated.

External stimuli can trigger reversible changes in the conformation of vinculin that alter its ability to bind to actin filaments and adhesion complex proteins (14, 28). The regulation of the vinculin head to tail interaction to expose or hide ligand-binding sites may be a mechanism for regulating connections between the cytoskeleton and integrin-talin adhesion junctions that control cell adhesion and motility (14, 31). Talin plays a key role in regulating the conformation of vinculin, and its binding to vinculin either alone or in combination with other ligands such as α-actinin, F-actin, and acidic phospholipids is required to convert vinculin from its closed inactive conformation to an open active conformation (29, 31–34). We therefore hypothesized that the formation of connections between integrin adhesion junctions and actin filaments by vinculin during the contractile stimulation of SMCs may be critical for the regulation of tension transmission from the contractile apparatus to the extracellular matrix.

Vinculin can undergo phosphorylation at several sites that may contribute to the regulation of its molecular function, including at Tyr-1065 on the C-terminal of its tail domain. Vinculin phosphorylation at Tyr-1065 might contribute to stabilizing its open conformation, or it may promote lipid interactions that contribute to vinculin activation (35). In the current study, we evaluated changes in vinculin phosphorylation at Tyr-1065 during the contractile stimulation of tracheal muscle tissues.

Vinculin may also participate in the coupling of actin polymerization to cell adhesion. The Arp2/3 complex, a key regulator of actin polymerization, transiently associates with activated vinculin (36). Vinculin also binds to paxillin, a cytoskeletal scaffolding protein that is involved in the regulation of cell motility and adhesion complex formation (37, 38). We previously found that paxillin phosphorylation at Tyr-31 and Tyr-118 regulates activation of the actin-nucleation initiator protein neuronal Wiskott-Aldrich Syndrome protein (N-WASp) in tracheal smooth muscle and that both paxillin tyrosine phosphorylation and N-WASp activation are required for the initiation of actin polymerization by the Arp2/3 complex in response to a contractile stimulus (8). Paxillin and vinculin are both recruited to the SMC membrane in response to a contractile stimulus (26). Thus, we hypothesized that the recruitment of vinculin to cell adhesion junctions may be critical for paxillin- or vinculin-mediated initiation of actin polymerization.

The overall goal of the current study was to determine whether contractile stimuli regulate the activation state of vinculin and its molecular functions in tracheal smooth muscle and whether the regulation of vinculin activity during contractile stimulation plays an important role in active tension development. Our results indicate that the activation of vinculin and its interaction with talin at the membrane are regulated by contractile stimulation in smooth muscle and that vinculin activation may contribute to the formation of linkages between integrin adhesion complexes and filamentous actin. Furthermore, we found that vinculin activation is required for stimulus-induced paxillin phosphorylation and the initiation of actin polymerization in response to a contractile stimulus in airway smooth muscle and that vinculin activation is necessary for active tension development.

EXPERIMENTAL PROCEDURES

Reagents and Antibodies—Antibodies: Rabbit anti-phospho-vinculin site-specific (pY1065) (Invitrogen); Mouse anti-paxillin (BD Biosciences Pharmingen); rabbit polyclonal anti-phospho-paxillin tyrosine Y118 (BIOSOURCE); vinculin C-terminal (C-20) (Santa Cruz Biotechnology); vinculin N-terminal (Vin-11–5), talin (Sigma); Alexa Fluor 488 and 546 (Invitrogen). Polyclonal vinculin (against canine cardiac vinculin) and myosin light chain monoclonal antibody were custom made by BABCO (Richmond, CA). Duolink *in situ* proximity ligation assay kit (PLA) and Duolink anti-mouse Plus, anti-rabbit Minus, and anti-goat Minus probes (Olink Bioscience, Uppsala, Sweden).

Plasmids encoding full-length chicken vinculin (residues 1–1066), pEGFP-vinculin, vinculin head domain (residues 1–851) pEGFP-Vh, and the talin-binding deficient vinculin head domain mutant pEGFP-VhA50I (residues 1–851 with site mutation A50I) were provided by Dr. Susan Craig (32). pFLAG-Vh was constructed by subcloning the EcoRI/SalI fragment of pEGFP-Vh into pFLAG-CMV-2 mammalian expression vector (Sigma) at EcoRI/SalI sites. The cDNAs encoding the human HA-RhoA Asn-19 mutant were subcloned into the mammalian expression vector pcDNA 3.1 (39).

Preparation of Smooth Muscle Tissues and Measurement of Force—Mongrel dogs (20–25 kg) were euthanized in accordance with procedures approved by the Institutional Animal Care and Use Committee of Indiana University School of Medicine. Smooth muscle strips (1 × 0.2–0.5 × 15 mm) were dissected from tracheal segments, cleaned of connective and epithelial tissues, attached to force transducers, and maintained in an organ chamber in physiological saline solution at 37 °C for the measurement of contractile force.

Transfection of Smooth Muscle Tissues—Plasmids encoding recombinant vinculin proteins were introduced into tracheal smooth muscle tissue strips by the method of reversible permeabilization (8, 26, 40, 41). Tissues were incubated successively in each of the following solutions: solution 1, which contained 10 mM EGTA, 5 mM Na_2ATP, 120 mM KCl, 2 mM $MgCl_2$, and 20 mM TES (at 4 °C, pH 7.1, 100% O_2 for 120 min); solution 2, which contained 0.1 mM EGTA, 5 mM Na_2ATP, 120 mM KCl, 2 mM $MgCl_2$, 20 mM TES, and 10 μg of plasmids (at 4 °C, pH 7.1, 100% O_2 overnight); solution 3, which contained 0.1 mM EGTA, 5 mM Na_2ATP, 120 mM KCl, 10 mM $MgCl_2$, and 20 mM TES (at 4 °C, pH 7.1, 100% O_2 for 30 min); and solution 4, which contained 110 mM NaCl, 3.4 mM KCl, 0.8 mM $MgSO_4$, 25.8 mM $NaHCO_3$, 1.2 mM KH_2PO_4, and 5.6 mM dextrose (at 22 °C, pH 7.4, 95% O_2, 5% CO_2 for 60 min). After 30 min in solution 4, $CaCl_2$ was added gradually to reach a final concentration of 2.4 mM. The strips were then incubated in a CO_2 incubator at 37 °C for 2 days in serum-free DMEM containing 5 mM Na_2ATP, 100 units/ml penicillin, 100 μg/ml streptomycin, and 10 μg/ml plasmids to allow for expression of the recombinant proteins. Sham-treated tissues were subjected to identical procedures except that no plasmids were included in solution 2.

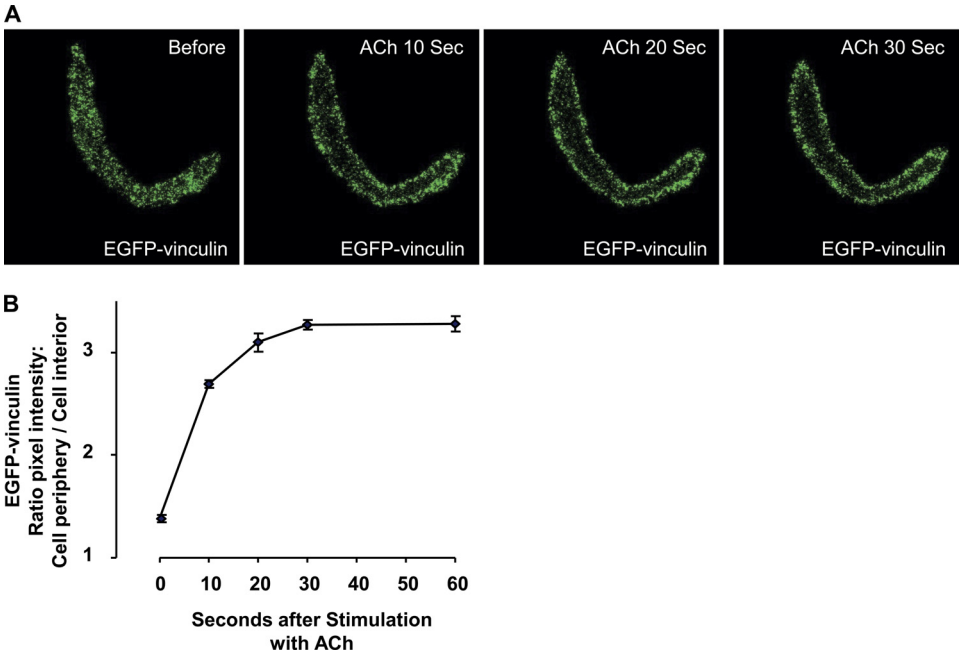

FIGURE 1. **Contractile stimulation with ACh induces the rapid recruitment of recombinant EGFP-vinculin to the cell membrane.** The cells were enzymatically dissociated from smooth muscle tissue strips expressing EGFP-vinculin. The localization of EGFP-vinculin was monitored by confocal microscopy during stimulation with 10^{-4} M ACh. *A*, images are shown before ACh and 10, 20, and 30 s after ACh (see also supplemental Movie S1). *B*, mean changes in EGFP-vinculin localization in six living cells during 60 s of stimulation with 10^{-4} M ACh. The values are the means ± S.E. of ratios of fluorescence signal pixel intensity from cell membrane to cell interior.

Cell Dissociation, Live Cell Imaging, and Immunofluorescence Analysis—Primary cells were used for these studies to prevent morphological changes in cytoskeletal organization that occur during the culture of SMCs. SMCs were enzymatically dissociated from tracheal muscle strips (8, 26). Freshly dissociated cells were plated onto glass coverslips and allowed to adhere for 30–60 min. The localization of EGFP-vinculin was monitored immediately in live cells during contraction with 100 μM ACh by using a Zeiss LSM 510 or an Olympus Fluoview FV1000 confocal microscope. Consistent with our previous reports (8, 26, 41), recombinant protein expression was observed in ~90% of the freshly dissociated cells.

Freshly dissociated SMCs were also fixed and stained for immunofluorescence analysis. Regional differences in cellular localization of specific proteins were evaluated by quantifying the pixel intensity of fluorescent signals with a series of cross-sectional line scans along the entire length of each cell excluding the nucleus (8, 26). The ratio of pixel intensity between the cell periphery and the cell interior was computed for each line scan and averaged to obtain a single value for each cell.

In Situ Proximity Ligation Assay—Duolink™ *in situ* proximity ligation assay (PLA) (Olink Bioscience, Uppsala, Sweden) was performed to detect interactions between talin and vinculin (42). PLA yields a fluorescent signal (fluorescent spot) when the target proteins are localized within 40 nm of each other. Dissociated cells were fixed, permeabilized, and incubated with primary antibodies against talin and vinculin. A pair of oligonucleotide-labeled secondary antibodies (PLA probes) were targeted to primary antibodies to talin and vinculin. Duolink hybridization, ligation, amplification, and detection media were administered according to the manufacturer's instructions. Randomly selected cells from both unstimulated and ACh-stimulated groups were analyzed for talin-vinculin interactions by counting Duolink fluorescent spots using a Zeiss LSM510 confocal microscope.

Immunoblot and Immunoprecipitation—Frozen muscle tissues were pulverized, and the proteins were extracted for electrophoresis or immunoprecipitation (8, 12, 43). For immunoprecipitation, the extracts were precleared at 4 °C with protein A/G UltraLink Resin and incubated with primary antibodies. Protein extracts or immunoprecipitates were separated by SDS-PAGE, transferred to nitrocellulose, and probed with antibodies against proteins of interest followed by horseradish peroxidase-conjugated IgG (Amersham Biosciences). The proteins were visualized by ECL and digitally quantified using a Bio-Rad ChemiDoc XRS detection system. Recombinant vinculin head domain expression was analyzed by two-dimensional PAGE as described previously (44).

MLC Phosphorylation—Frozen muscle strips were immersed in dry ice-precooled acetone containing 10% (w/v) trichloroacetic acid and 10 mM dithiothreitol. The proteins were extracted using an 8 M urea buffer. Phosphorylated and unphosphorylated MLCs were separated by glycerol-urea polyacrylamide gel electrophoresis, transferred to nitrocellulose, and then immunoblotted for MLC (6, 8, 12, 45). MLC and phosphorylated MLC were visualized by ECL and digitally quantified using a Bio-Rad ChemiDoc XRS detection system. The ratio of phosphorylated MLC to total MLC was calculated for each sample.

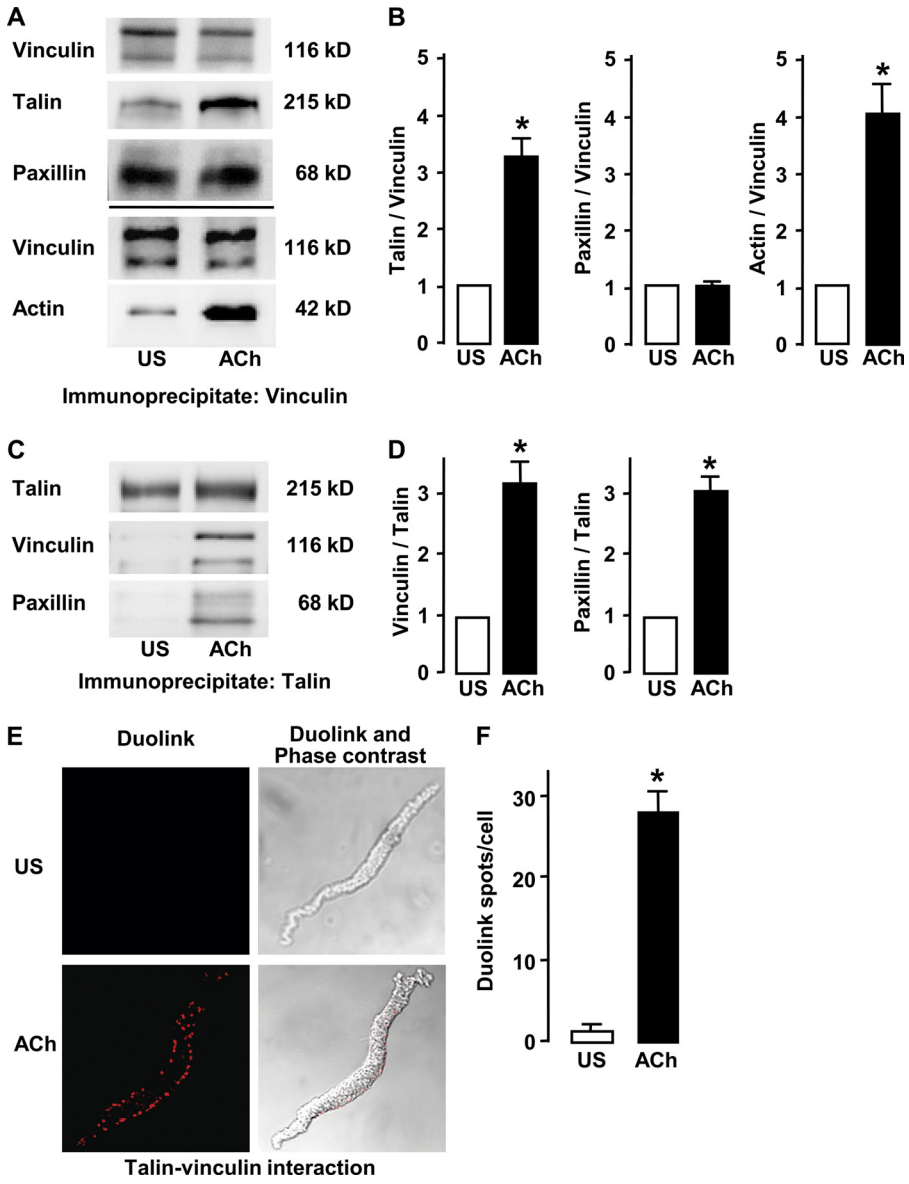

FIGURE 2. **The interaction of talin and actin with vinculin increases in response to contractile stimulation with ACh.** *A*, the amounts of talin and actin that co-immunoprecipitate with vinculin are significantly higher in ACh-stimulated tissues than in unstimulated (US) tissues, whereas similar amounts of paxillin co-immunoprecipitate with vinculin from ACh-stimulated and US tissues. *B*, mean relative amounts of talin, paxillin, and actin that co-precipitate with vinculin from extracts from US and ACh-stimulated muscle tissues ($n = 5$). *C*, more vinculin and paxillin co-immunoprecipitate with talin from ACh-stimulated tissues than from US tissues. *D*, mean relative amounts of vinculin and paxillin that co-precipitate with talin in extracts from US and ACh-stimulated muscle tissues ($n = 6$). *E*, interaction of talin and vinculin in freshly dissociated tracheal SMCs detected using the Duolink *in situ* proximity ligation assay is higher in ACh-stimulated cells than in US cells. *Left panels*, fluorescent images of cells treated with Duolink ligation probes to assess the interaction of vinculin and talin. *Right panels*, phase-contrast images of the same cells merged with fluorescent images. Each fluorescent spot indicates interaction between talin and vinculin. No signals are detected in US cells, whereas many spots are seen at the membrane of the ACh-stimulated cells. *F*, the total number of DuoLink spots was significantly higher in ACh-stimulated SMCs (27.8 ± 2.4, $n = 26$) than in unstimulated cells (1.2 ± 0.7, $n = 24$; the cells from three separate experiments). All of the values are the means ± S.E. *, significantly different from US tissues or cells with the same treatment ($p < 0.05$).

Analysis of F-actin and G-actin—The relative proportions of F-actin and G-actin were analyzed in smooth muscle tissues by fractionation using an assay kit from Cytoskeleton (Denver, CO) (8). The tracheal smooth muscle strips were homogenized in F-actin stabilization buffer. Supernatants of the protein extracts were collected after high speed centrifugation. The pellets were resuspended in 10 μM cytochalasin D and then incubated to depolymerize F-actin. The supernatant (G-actin) and pellet (F-actin) fractions were subjected to immunoblot analysis using anti-actin antibody (clone AC-40; Sigma). The ratios of F-actin to G-actin were quantified using a Bio-Rad ChemiDoc XRS digital detection system.

RESULTS

The Stimulation of Freshly Dissociated Tracheal SMCs with ACh Causes the Rapid Recruitment of EGFP-Vinculin to the Cell Periphery—Freshly dissociated SMCs from tissues expressing EGFP-vinculin were visualized live during stimulation with 10^{-4} M ACh. The cells were scanned for 5–10 s be-

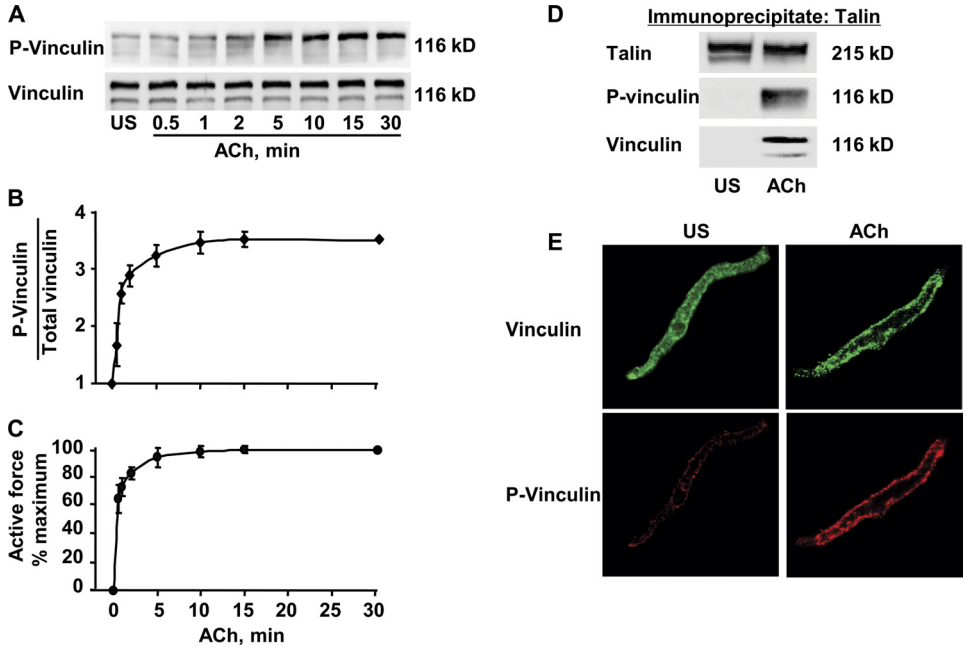

FIGURE 3. **Contractile stimulation increases vinculin phosphorylation at Tyr-1065 at the membrane of SMCs.** *A*, immunoblot of phospho-vinculin (Tyr-1065) and total vinculin in seven muscle tissue strips stimulated with ACh for 0.5, 1, 2, 5, 10, 15, or 30 min and one muscle strip without stimulation (US). *B* and *C*, mean increases in vinculin phosphorylation at Tyr-1065 and force in response to ACh. Vinculin phosphorylation is normalized to unstimulated tissues; forces are normalized to value at 30 min after ACh ($n = 4$). *D*, phospho-vinculin was detected in the talin immunoprecipitates from extracts of tissues stimulated with 10^{-4} M ACh but was not detected in the talin precipitated from unstimulated tissues. *E*, cells freshly dissociated from muscle tissues were stimulated with 10^{-4} M ACh or left unstimulated. *Red*, phospho-vinculin at Tyr-1065; *green*, total vinculin (polyclonal antibody). Vinculin is distributed throughout the cytoplasm in US cells and localizes to the cell periphery in ACh-stimulated cells. Phospho-vinculin localizes to cell periphery in both US and ACh-stimulated cells.

fore stimulation and for 30–60 s after stimulation (Fig. 1 and supplemental Movie S1). The plane of focus was adjusted to visualize a mid-section of each cell (supplemental Fig. S1). EGFP-vinculin fluorescence increased significantly at the cell periphery within 10 s after ACh stimulation and was maintained for the duration of the ACh stimulation period.

The Association of Vinculin with Talin and Actin Increases in Response to ACh Stimulation—We used co-immunoprecipitation analysis to evaluate the effect of ACh stimulation of tracheal smooth muscle tissues on the interactions of vinculin with talin, F-actin, and paxillin, a vinculin-binding protein (37). F-actin and talin bind preferentially to vinculin in the open conformation (29). The amounts of talin and actin were both higher in vinculin immunoprecipitates from ACh-stimulated tissues than in immunoprecipitates from unstimulated muscle tissues and more vinculin-immunoprecipitated with talin from ACh-stimulated tissues than from unstimulated tissues (Fig. 2, *A–D*).

A similar amount of paxillin was associated with vinculin precipitates from unstimulated and stimulated tissues. This observation is consistent with evidence that the binding of paxillin to vinculin does not depend on the conformation state of vinculin (46, 47). Vinculin and paxillin may be concurrently recruited to membrane adhesion junctions as a protein complex during contractile stimulation.

The effect of ACh stimulation on the interaction of vinculin with talin was further evaluated using a Duolink *in situ* PLA assay in freshly dissociated tracheal SMCs. The signals generated by the interaction of PLA probes targeted to talin and vinculin were quantitated in unstimulated and ACh-stimulated muscle cells. The average number of fluorescent spots was 27.8 ± 2.4 ($n = 26$) in ACh-stimulated SMCs compared with 1.2 ± 0.65 spots in unstimulated cells ($n = 26$), indicating a dramatic increase in the interaction of vinculin with talin at membrane sites caused by ACh stimulation.

Overall, these results provide strong evidence that the contractile stimulation of smooth muscle with ACh results in the recruitment of vinculin to the membrane and its conversion from a closed autoinhibited conformation to an open activated conformation that enables the interaction of vinculin with talin and actin.

The Stimulation of Muscle Tissues with ACh Induces a Time-dependent Increase in Vinculin Phosphorylation at Tyr-1065 and an Increase in Phosphovinculin at the Cell Membrane—We evaluated the time course of vinculin phosphorylation at Tyr-1065 in muscle tissues stimulated with ACh for 30 min. Vinculin phosphorylation increased concurrently with the onset of force development immediately after ACh stimulation and reached a maximum within 15 min (Fig. 3, *A–C*). Phospho-vinculin co-immunoprecipitated with talin from ACh-stimulated muscles but not from unstimulated muscles, indicating that the phosphorylated vinculin was associated with talin (Fig. 3*D*).

Phospho-vinculin at Tyr-1065 was also visualized by immunofluorescence in freshly dissociated tracheal SMCs (Fig. 3*E*). In unstimulated cells, a small amount of phospho-vinculin could be detected at the cell membrane, whereas unphosphorylated vinculin was distributed throughout the cytoplasm. In cells stimulated with ACh, the amount of vinculin and phosphovinculin at the cell

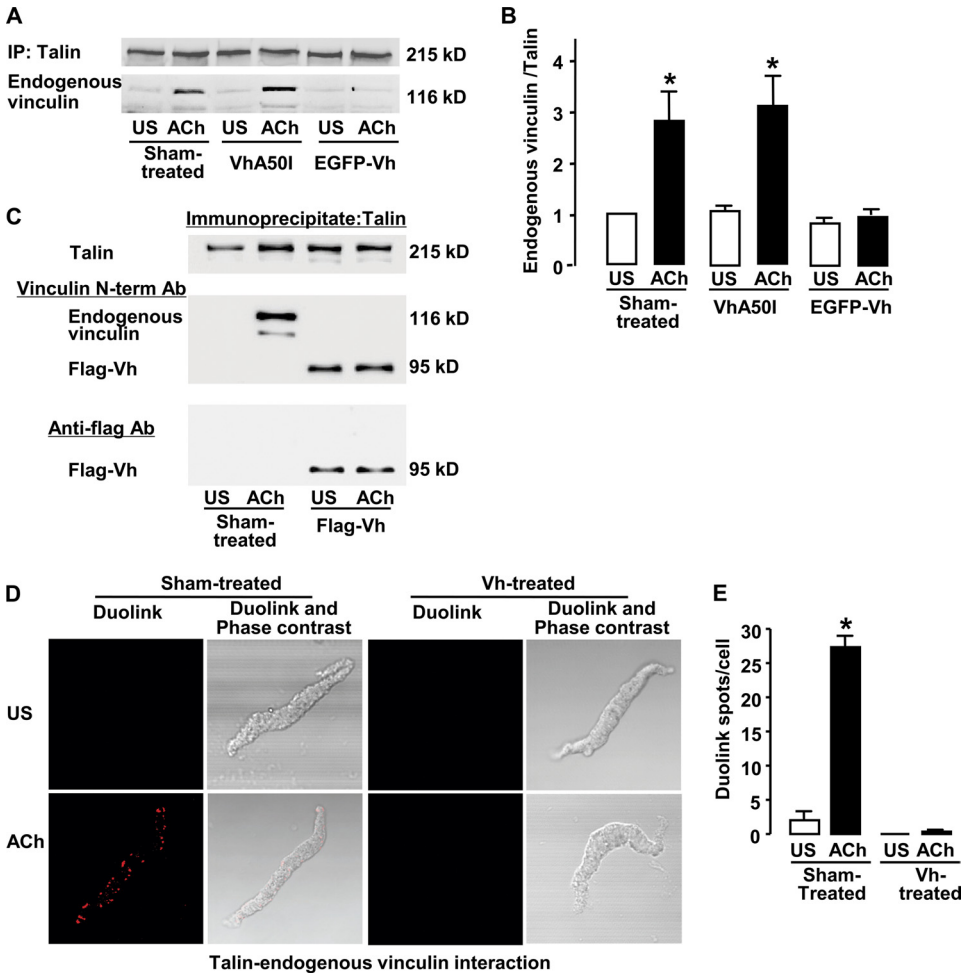

FIGURE 4. **Expression of EGFP-Vh or FLAG-Vh recombinant protein in tracheal smooth muscle decreases the interaction between endogenous vinculin and talin.** *A*, talin was immunoprecipitated (*IP*) from sham-treated, EGFP-VhA50I-treated, EGFP-Vh-treated tissues after 5 min of stimulation with 10^{-4} M ACh or without stimulation. Endogenous vinculin was detected with vinculin C-terminal antibody. In sham-treated and EGFP-VhA50I-treated tissues, more endogenous vinculin co-precipitated with talin in tissues stimulated with ACh. In EGFP-Vh-treated tissues, ACh stimulation did not increase the amount of endogenous vinculin that co-precipitated with talin. *B*, means ± S.E. relative amounts of endogenous vinculin that co-precipitated with talin from each treatment group. *, significant difference between ACh-stimulated and US tissues ($n = 4$, $p < 0.05$). *C*, talin was immunoprecipitated from sham-treated and FLAG-Vh-treated tissues stimulated with 10^{-4} M ACh or left unstimulated. Endogenous and recombinant vinculin proteins were detected with vinculin N-terminal and anti-FLAG monoclonal antibody. Endogenous vinculin co-precipitated with talin only in the ACh-stimulated sham-treated tissues but not in the FLAG-Vh-treated tissues. FLAG-Vh but not endogenous vinculin was detected in talin immunoprecipitates from both ACh-stimulated or unstimulated tissues using both vinculin N-terminal and anti-FLAG antibodies. *D*, expression of the Vh head domain in tracheal smooth muscle tissues inhibited the ACh-stimulated increase in interaction between talin and endogenous vinculin, as indicated by Duolink *in situ* proximity ligation assay performed on freshly dissociated cells. Each fluorescent spot indicates interaction between talin and endogenous vinculin. *Left panels*, sham-treated cells unstimulated (*US*) or stimulated with ACh. *Right panels*, ACh-stimulated cells and unstimulated (*US*) cells expressing vinculin Vh peptides. *E*, the total number of Duolink spots was significantly higher in sham-treated ACh-stimulated smooth muscle cells (US, $n = 29$; ACh, $n = 42$) than in cells expressing Vh peptides (US, $n = 18$; ACh, $n = 27$). All of the values are the means ± S.E. *, significantly different from US tissues or cells with the same treatment ($p < 0.05$).

membrane increased markedly. These results suggest that vinculin undergoes Tyr-1065 phosphorylation in SMCs in association with its recruitment to the membrane and interaction with talin at adhesion complexes.

Expression of Vh Decreases the Association of Vinculin with Talin—The truncated Vh can compete with endogenous vinculin for binding to talin (29) and thereby inhibit its activation. In contrast, a talin-binding-deficient vinculin mutant head domain peptide (EGFP-VhA50I) is identical to the EGFP-Vh except that it has a substitution of alanine for isoleucine at residue 50 within the talin-binding site that dramatically weakens its affinity for talin (14). Because VhA50I does not bind easily to talin, it should not compete with endogenous vinculin for talin binding and should therefore not inhibit endogenous vinculin activation (14, 29).

We expressed the truncated head domain of vinculin (EGFP-Vh or FLAG-Vh peptides) and EGFP-VhA50I in tracheal smooth muscle tissues. The expression of the recombinant vinculin proteins in the tracheal muscle tissues was confirmed by immunoblot (Fig. 4*C*), by analysis of immunofluorescence images of dissociated cells (Fig. 5*C*), and by two-dimensional gel electrophoresis of extracts from transfected tissues (supplemental Fig. S2). A polyclonal or N-terminal vinculin antibody was used to detect all vinculin species, and a vinculin C-terminal antibody was used to selectively detect endogenous vinculin (Figs. 4–6). In preliminary experiments, we confirmed that the polyclonal vinculin antibody reacted with both full-length recombinant vinculin (His-Vin1–1066) and the vinculin head domain peptide (His-Vh1–851), but the vinculin C-terminal antibody (C20) reacted only

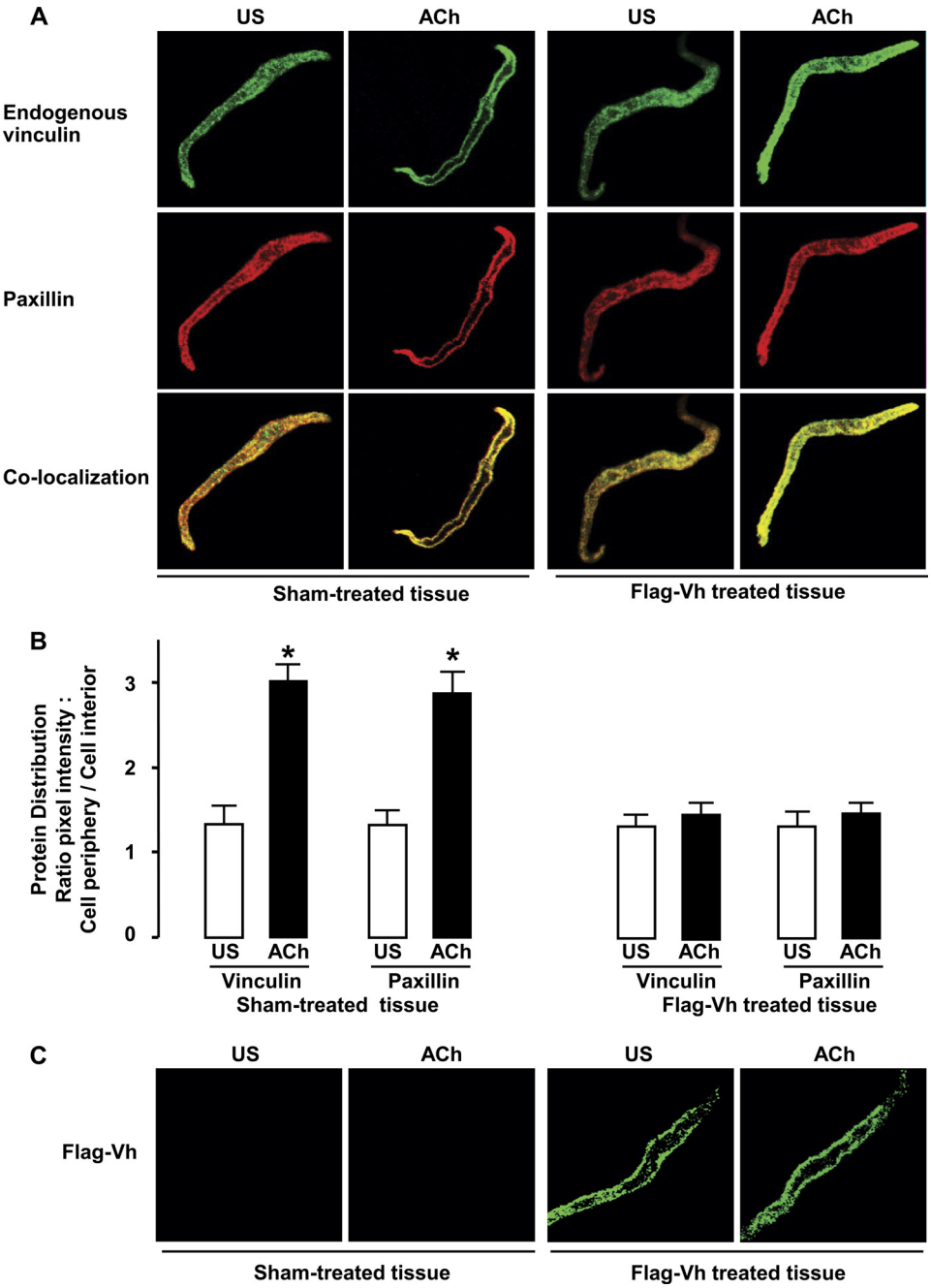

FIGURE 5. **FLAG-Vh inhibits the recruitment of endogenous vinculin and paxillin to the cell periphery.** *A*, dissociated SMCs from sham-treated tissues and FLAG-Vh-transfected tissues were stimulated with 10^{-4} M ACh or left US and then immunostained for endogenous vinculin (*green*) and paxillin (*red*). In sham-treated tissues, endogenous vinculin and paxillin were co-localized throughout the cell and increased their localization at the cell membrane in ACh-stimulated cells. In cells from FLAG-Vh-treated tissues, endogenous vinculin and paxillin did not increase their localization at the cell membrane in ACh-stimulated cells. *B*, mean ratios of pixel intensity at the cell periphery to cell interior for both vinculin and paxillin (30–35 cells from three experiments). *, significant difference between ACh-stimulated and US cells ($p < 0.05$). *C*, cells from sham-treated and FLAG-Vh-transfected tissues immunostained for FLAG-Vh using anti-FLAG antibody. FLAG-Vh was detected at the cell membrane in both US and ACh-stimulated cells from FLAG-Vh tissues.

with full-length vinculin (His-Vin1–1066) and not with vinculin head domain peptides (data not shown). The EGFP-Vh peptide could not be easily distinguished from endogenous vinculin using one-dimensional gel electrophoresis because the molecular weight of the EGFP-Vh protein is close to that of endogenous vinculin; therefore, FLAG-Vh was expressed in the tissues in some experiments because its electrophoretic mobility is clearly distinct from endogenous vinculin (Fig. 4*C*). EGFP-Vh and FLAG-Vh peptides were expressed in robust amounts approximately comparable with that of endogenous vinculin or metavinculin (Fig. 4*C* and supplemental Fig. S2).

We evaluated the effects of the Vh and VhA50I peptides on the interaction of vinculin and talin caused by stimulation with ACh (Fig. 4). In sham and EGFP-VhA50I-treated muscles, the amount of endogenous vinculin that co-precipitated with talin increased significantly in response to ACh stimulation. In contrast, in EGFP-Vh- or FLAG-Vh-transfected muscles, stimulation with ACh did not increase in the amount of

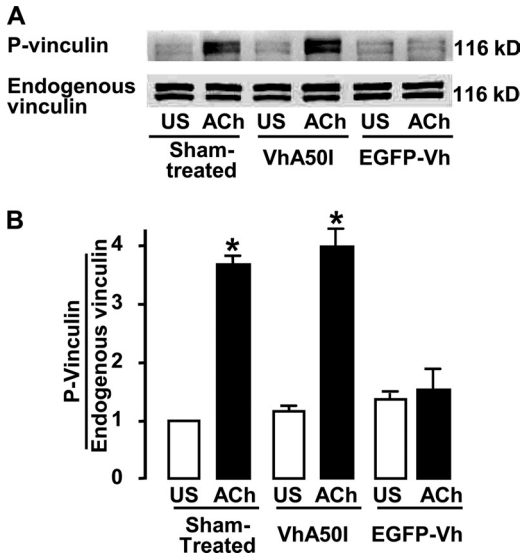

FIGURE 6. **EGFP-Vh inhibited endogenous vinculin phosphorylation at Tyr-1065 in response to ACh.** *A*, immunoblots of phospho-vinculin and endogenous vinculin (C-terminal antibody) in sham-, VhA50I-, and EGFP-Vh-treated muscle tissues. Vinculin phosphorylation increased in ACh-stimulated tissues from sham and VhA50I-treated tissues but not in Vh-treated tissues. *B*, mean ratios of phospho-vinculin over total endogenous vinculin from each treatment. The phospho-vinculin in stimulated tissues from sham-treated and VhA50I-treated groups was significantly higher than in unstimulated tissues; there was no significant difference in phospho-vinculin in unstimulated and ACh-stimulated tissues in Vh-treated tissues (means ± S.E.). *, significant difference between ACh and US tissues ($n = 5, p < 0.05$).

endogenous vinculin that co-precipitated with talin (Fig. 4, *A–C*). The FLAG-Vh protein co-precipitated with talin in both ACh-stimulated and unstimulated muscle tissues, but no endogenous vinculin was associated with talin in these tissues (Fig. 4*C*). The amount of vinculin that co-precipitated with talin in unstimulated muscles was not significantly different in the three groups. Our observation that expression of the talin binding-deficient Vh domain, EGFP-VhA50I, does not inhibit the increase in the association of endogenous vinculin with talin in ACh-stimulated muscles (Fig. 4*A*) confirms that the Vh head domain protein inhibits the association between talin and endogenous vinculin by competing with endogenous vinculin for talin binding.

Duolink proximity ligation assays were performed on freshly dissociated tracheal SMCs to evaluate the interaction of vinculin with talin and to determine the localization of vinculin/talin protein complexes (Fig. 4*D*). ACh-stimulated cells expressing EGFP-Vh exhibited very few Duolink spots, indicating few talin-vinculin interactions (0.26 ± 0.2, $n = 27$) compared with sham-treated cells (27.3 ± 1.7, $n = 42$). (The cells are from three separate experiments). Thus, expression of the Vh domain peptide competitively inhibited the increase in the interaction of endogenous vinculin and talin at the membrane sites in response to stimulation with ACh.

Expression of FLAG-Vh in Tracheal Muscle Tissues Inhibits the Localization of Endogenous Vinculin and Paxillin to the Cell Periphery—We used immunofluorescence analysis to evaluate the effect of expressing the vinculin Vh peptide on the localization of endogenous vinculin and paxillin and on their recruitment to the cell membrane in response to ACh stimulation (Fig. 5). SMCs were dissociated from FLAG-Vh and sham-treated muscle tissues, stimulated with ACh or left unstimulated, and then stained for paxillin and endogenous vinculin using the C-terminal vinculin antibody (C20). The distribution of vinculin and paxillin was evaluated by analyzing the ratio of pixel intensity between the cell membrane and the cytoplasm in mid-sections of the cell (supplemental Fig. S1).

In sham-treated SMCs, stimulation with ACh caused the recruitment of vinculin and paxillin to the membrane. In untreated unstimulated SMCs, the pixel intensity ratio for both vinculin and paxillin was 1.3 ± 0.2 and increased ~3-fold after ACh stimulation (Fig. 5, *A* and *B*). In SMCs from tissues expressing the FLAG-Vh peptide, the distribution of endogenous vinculin was unaffected by ACh stimulation and was similar to that of unstimulated cells from untreated tissues (Fig. 5, *A* and *B*). The FLAG-Vh peptide localized to the membrane in both unstimulated cells and cells stimulated with ACh (Fig. 5*C*). The expression of full-length recombinant vinculin protein (FLAG-WT-vinculin) did not inhibit the recruitment of endogenous vinculin to the membrane in response to ACh (supplemental Fig. S3). These results provide further evidence that the expression of Vh head domain peptide inhibits the recruitment of endogenous vinculin to the membrane in response to ACh stimulation. We also noticed that dissociated cells from FLAG-Vh-treated tissues took significantly longer to attach to the glass coverslips (40–60 min) than cells from sham-treated tissues (10–30 min), suggesting that the expression of the Vh peptide impaired adhesion processes in these cells.

Expression of EGFP-Vh Decreases the Phosphorylation of Endogenous Vinculin on Tyrosine 1065—We expressed EGFP-Vh and EGFP-VhA50I in smooth muscle tissues and evaluated their effects on endogenous vinculin phosphorylation at Tyr-1065 in response to ACh (Fig. 6). Endogenous vinculin phosphorylation at Tyr-1065 increased significantly in response to ACh in sham-treated (3.7 ± 0.1-fold) and EGFP-VhA50I-treated tissues (4.0 ± 0.5-fold) but not in EGFP-Vh-treated tissues (1.3 ± 0.6-fold). Because endogenous vinculin was inhibited from talin binding in EGFP-Vh-treated tissues, these results suggest that vinculin phosphorylation at Tyr-1065 occurs in response to ACh stimulation only when vinculin is activated by talin binding.

Expression of EGFP-Vh Inhibits Force Development in Smooth Muscle Tissues—The effect of inhibiting vinculin activation on force development in response to ACh stimulation was evaluated by expressing EGFP-Vh and VhA50I in tracheal smooth muscle tissues (Fig. 7). EGFP-Vh decreased contractile force to 38 ± 3% of force in sham-treated tissues, whereas expression of EGFP-VhA50I did not significantly affect contractile force (103 ± 5%) ($n = 14, p < 0.05$).

Expression of EGFP-Vh Does Not Affect MLC Phosphorylation—We evaluated the possibility that vinculin activation contributes to the regulation of phosphorylation of the 20-kDa regulatory MLC, which is critical for the activation of actomyosin cross-bridge cycling and tension development in smooth muscle (2). MLC phosphorylation increased significantly in response to ACh stimulation in sham-treated, EGFP-vinculin WT, and EGFP-Vh-treated muscle tissues and

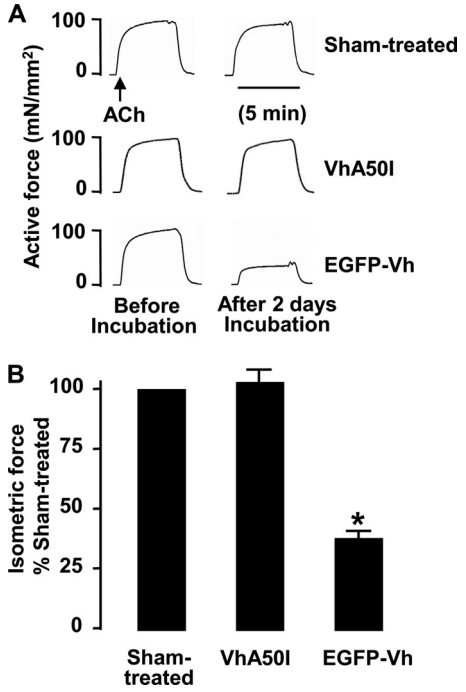

FIGURE 7. **Effect of expression of EGFP-Vh on force in tracheal smooth muscle tissues stimulated with 10^{-5} M ACh under isometric conditions.** *A*, representative isometric contractions in response to ACh stimulation in three muscles from one experiment. Contractions were measured before and after transfection of tissues with plasmids encoding EGFP-Vh or EGFP-VhA50I and 2-day incubation for expression of recombinant proteins. Sham-treated muscles were subjected to same procedures without plasmids. Contractile force in response to ACh stimulation was dramatically inhibited in tissues treated with EGFP-Vh, but the force was not depressed in sham-treated or EGFP-VhA50I-treated tissues. *B*, mean ± S.E. of force in response to 10^{-5} M ACh quantified as the percentage of force in sham-treated tissues. *, significant difference between sham-treated and plasmid-transfected tissues ($n = 14$, $p < 0.05$).

was not significantly affected by expression of either WT vinculin or EGFP-Vh (Fig. 8, *A* and *B*; $n = 4$, $p > 0.05$). However, contractile force in the EGFP-Vh-treated tissues was significantly depressed to 41 ± 5% of that in sham-treated muscles ($n = 4$, $p < 0.05$) (Fig. 8, *C* and *D*). Thus, vinculin activation does not contribute to the regulation of pathways that mediate MLC phosphorylation, and the inhibitory effect of Vh on contraction is not due to the disruption of pathways that regulate MLC phosphorylation.

Inhibition of MLC Phosphorylation Does Not Affect the ACh-stimulated Increase in Vinculin/Talin Interaction or Vinculin Phosphorylation at Tyr-1065—We evaluated the possibility that activation of vinculin might be stimulated by actomyosin activity and tension development. Tracheal smooth muscle tissues were treated with the MLC kinase inhibitor ML-7 to inhibit MLC phosphorylation and thereby suppress actomyosin cross-bridge cycling. We have previously shown that 30 μM ML-7 inhibits ACh-induced contractile force by 60–70% and suppresses ACh-induced MLC phosphorylation to close to basal levels (12). In the present study, treatment of the tissues with ML-7 had no significant effect on the ACh-stimulated increase in the interaction of vinculin and talin; nor did it affect vinculin phosphorylation at Tyr-1065. Thus, ACh-induced vinculin activation does not depend on myosin activation or tension development (Fig. 9).

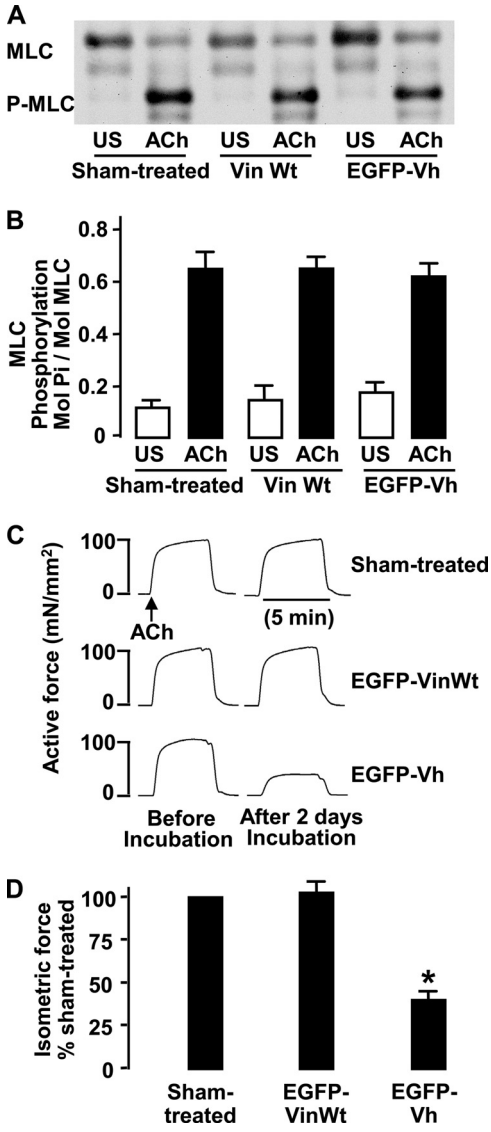

FIGURE 8. **Expression of EGFP-Vh does not inhibit the increase in MLC phosphorylation in response to ACh stimulation.** Muscle tissues from sham-treated, EGFP-VinWt-treated, and EGFP-Vh-treated muscles were stimulated with 10^{-4} M ACh for 5 min or left unstimulated. Isometric force was measured, and tissues were frozen for the measurement of MLC phosphorylation. *A*, immunoblot of unphosphorylated and phosphorylated MLC (20 kDa) in US and ACh-stimulated muscle tissues from each treatment group. *B*, MLC phosphorylation increased significantly in response to ACh in all treatment groups, but it was not significantly different among tissues subjected to different treatments ($n = 4$, $p < 0.05$). *C*, representative isometric contractions in response to ACh stimulation in sham-treated, EGFP-VinWt-treated, and EGFP-Vh-treated muscles. *D*, mean isometric force from muscles showing significant force depression of EGFP-Vh group. *, means ± S.E., significantly different from sham-treated tissues ($n = 4$, $p < 0.05$).

Expression of EGFP-Vh Inhibits the Increase in Actin Polymerization in Response to Contractile Stimulation with ACh—The polymerization of a small pool of actin is required for contraction and force development in tracheal smooth muscle tissues, and the pathways that regulate actin polymerization are distinct from those that regulate MLC phosphorylation (3, 4, 12). In tracheal smooth muscle, actin polymerization is catalyzed by an array of proteins that localize to membrane adhesion complexes (3, 8, 12, 40, 43). We evaluated the effect of inhibiting vinculin activation on the ACh-

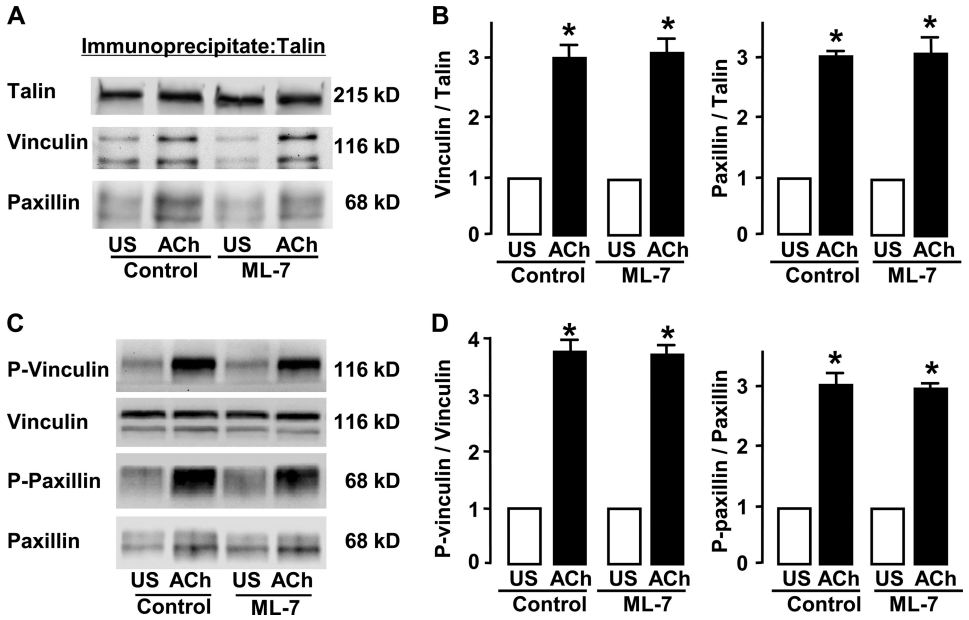

FIGURE 9. **Inhibition of MLC phosphorylation with ML-7 does not inhibit the association between vinculin and talin induced by ACh, vinculin phosphorylation at Tyr-1065, or paxillin phosphorylation at Tyr-118.** *A*, muscle tissues were incubated with 30 μM ML-7 or untreated (control) and stimulated with ACh 10^{-4} M for 5 min or left US, and the co-immunoprecipitation of vinculin and paxillin with talin was analyzed by immunoblot. *B*, means ± S.E. relative amounts of vinculin and paxillin that co-precipitated with talin from each treatment group. ML-7 had no significant effect on the increase in the co-immunoprecipitation of vinculin and paxillin with talin in response to ACh. *, significant difference between ACh-stimulated and US tissues ($n = 4$, $p < 0.05$). *C*, immunoblot of phospho-vinculin (Tyr-1065), total vinculin, phospho-paxillin (Tyr-118), and total paxillin in ML-7-treated muscle tissue strips and untreated muscle strips stimulated with ACh and US. *D*, treatment with ML-7 had no significant effect on the phosphorylation of vinculin Tyr-1065 and paxillin Tyr-118 in response to ACh ($n = 4$, $p < 0.05$).

induced increase in polymerized actin in tracheal muscle tissues by determining the ratio of F-actin to G-actin in extracts from unstimulated and stimulated muscle tissues that had been transfected with EGFP-Vh or EGFP-VhA50I or were sham-treated. ACh stimulation significantly increased the F-actin/G-actin ratio in both sham-treated and EGFP-VhA50I-treated tissues, but expression of the EGFP-Vh protein significantly inhibited the increase in the F-actin/G-actin ratio caused by ACh stimulation ($p < 0.05$, $n = 5$). The ratios of F-actin/G-actin in unstimulated muscles were unaffected by their treatment (Fig. 10).

Expression of EGFP-Vh Decreases Paxillin Phosphorylation—In tracheal smooth muscle tissues, paxillin phosphorylation at Tyr-118 occurs in response to contractile stimulation and is a critical step in the regulation of N-WASp-mediated actin polymerization (3, 40, 43, 48). Vinculin binds to paxillin in its tail domain (49) and co-localizes with paxillin at membrane adhesion junctions (26, 37, 47, 50). EGFP-Vh lacks the paxillin-binding domain and therefore cannot bind to paxillin. We therefore evaluated whether expression of the Vh peptide in tracheal muscle tissues inhibits the recruitment of paxillin to membrane adhesion sites and its phosphorylation at Tyr-118 (Fig. 11).

Stimulation with ACh caused a significant increase in paxillin phosphorylation in sham-treated and EGFP-VhA50I tissues, but the ACh-induced increase in paxillin phosphorylation was inhibited in tissues expressing EGFP-Vh ($n = 5$, $p < 0.05$). In unstimulated muscles, paxillin phosphorylation was unaffected by treatment of the muscles. Thus, the inhibition of ACh-induced paxillin phosphorylation by the Vh peptide could disrupt tension

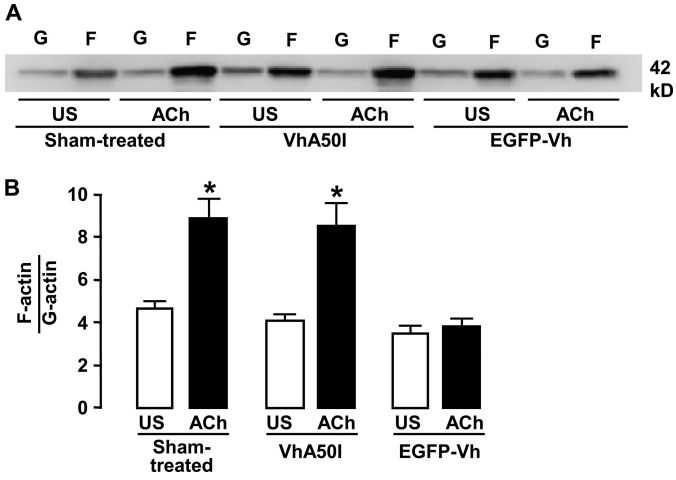

FIGURE 10. **Effect of expression of EGFP-Vh on the increase in F-actin/G-actin ratio in response to ACh stimulation in tracheal muscle tissues.** *A*, representative immunoblot showing actin from soluble (G-actin) and insoluble (F-actin) fractions obtained from one experiment on six muscle strips. G-actin was lower and F-actin was higher after stimulation with ACh in sham-treated or EGFP-VhA50I-treated tissues. *B*, mean ratios of F-actin/G-actin. Expression of EGFP-Vh inhibited the increase in F-actin/G-actin ratio in response to ACh stimulation (means ± S.E.). *, significant difference between ACh-stimulated and unstimulated tissues in same treatment group ($n = 5$, $p < 0.05$).

development by disrupting pathways leading to N-WASp-mediated actin polymerization.

Inhibition of RhoA Activation Suppresses ACh-induced Vinculin Activation in Tracheal Smooth Muscle Tissues—ACh stimulation of tracheal smooth muscle causes the activation of the small GTPase RhoA, which is required for contraction and ACh-induced actin polymerization (12). Expression of the

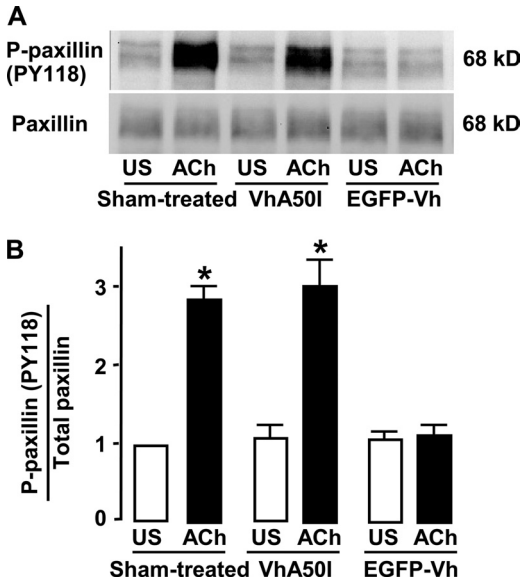

FIGURE 11. **Expression of EGFP-Vh inhibits paxillin phosphorylation in tracheal smooth muscle tissues.** *A*, immunoblot showing that paxillin Tyr-118 phosphorylation was higher in extracts from ACh-stimulated sham-treated or EGFP-VhA50I-transfected muscle tissues relative to unstimulated tissues. The paxillin Tyr-118 phosphorylation level was similar in extracts from unstimulated and ACh-stimulated tissues in the EGFP-Vh-transfected group. *B*, mean paxillin Tyr-118 phosphorylation did not increase after ACh stimulation in EGFP-Vh-transfected tissues (means ± S.E.). *, significant difference between ACh-stimulated and unstimulated tissues ($n = 5$, $p < 0.05$).

dominant negative inactive RhoAT19N inhibits ACh-induced RhoA activation and suppressed tension development in this tissue (Fig. 12).

We introduced RhoAT19N into tracheal smooth tissues to determine the role of RhoA in the regulation of ACh-induced vinculin activation. Vinculin activation in response to ACh was inhibited in tissues treated with RhoAT19N, as indicated by significantly less co-immunoprecipitation of vinculin and paxillin with talin and lower levels of vinculin phosphorylation (Fig. 12, *A–D*). Furthermore, Duolink PLA analysis revealed very few ACh-stimulated vinculin/talin interactions in RhoA-inactivated cells (1.2 ± 0.6 spots, $n = 30$) in contrast to sham-treated cells, which exhibited many interactions (30.4 ± 3.8 spots, $n = 34$) (Fig. 12, *E* and *F*). These results suggest that RhoA mediates the ACh-stimulated activation of vinculin in tracheal smooth muscle tissues.

DISCUSSION

Our results provide the first demonstration that the contractile stimulation regulates the interaction of vinculin with talin and actin at adhesion junctions in smooth muscle and that the regulation of vinculin activity plays an important role in the development of active tension in this tissue. Live cell imaging of EGFP-vinculin and immunofluorescence images of endogenous vinculin demonstrated that vinculin was recruited to the membrane of freshly isolated SMCs within seconds after contractile stimulation (Fig. 1 and supplemental Movie S1 and Fig. 5*A*). The time course of vinculin recruitment in response to ACh is similar to what we have observed for other adhesion complex proteins in response to contractile stimulation of these cells (41). Evaluation of the interaction of talin and vinculin by co-immunoprecipitation and Duolink PLA analysis provided strong evidence that the coupling of vinculin to talin and actin markedly increases in response to ACh (Fig. 2). Because vinculin is inhibited from binding to talin and actin when it is in the autoinhibited "closed" state (28), these results indicate that ACh stimulation catalyzes the conversion of a pool of autoinhibited vinculin to the "open" activated state in which it binds to talin and actin and that this activated vinculin resides at adhesion junctions (Fig. 13).

The phosphorylation of vinculin on its C-terminal Tyr-1065 increased at the onset of contractile stimulation and was maintained for the duration of the stimulation period. Phosphorylated vinculin could be detected only at the membrane of the SMCs (Fig. 3). Although the function of vinculin phosphorylation at this site is unclear, Zhang *et al.* (35) proposed that it might contribute to stabilizing the open conformation of vinculin after its activation by ligands such as talin and α-actinin or that it might promote membrane lipid interactions that contribute to vinculin activation. They found that platelet stimulation elicits vinculin phosphorylation by c-Src on the vinculin C-terminal Tyr-1065 and affects cell spreading and observed little or no vinculin phosphorylation in unstimulated platelets (35). Furthermore, *in vitro* analysis of the binding interactions of phosphorylated and unphosphorylated vinculin tail domain peptides suggested that the C-terminal tyrosine residue might be inaccessible to Src kinase in intact vinculin. Analysis of the crystal structure of vinculin suggests that access to the C terminus may be occluded in intact autoinhibited vinculin (28, 51). Our observations that the Tyr-1065 phosphorylation of vinculin at the membrane increases in ACh-stimulated SMCs are consistent with the possibility that the phosphorylation of vinculin is associated with its conversion to an open conformation.

We expressed the vinculin head domain peptide (EGFP-Vh or FLAG-Vh) in smooth muscle tissues with the objective of inhibiting vinculin activation (Fig. 4). The Vh peptide cannot assume an autoinhibited conformation because it lacks the tail domain (14, 32). Because the talin-binding sites on the truncated Vh protein remain exposed, it has much higher affinity for talin than full-length vinculin (32). However, without the actin-binding site on the tail domain, when truncated Vh binds to talin, it cannot form links between adhesion complexes and actin filaments (Fig. 13).

Our results provide strong evidence that expression of the Vh peptide in tracheal smooth muscle inhibits the activation of endogenous vinculin in response to ACh and that the binding of vinculin to talin is necessary for vinculin activation. Using co-immunoprecipitation and the Duolink *in situ* proximity ligation assay, we demonstrated that expression of the Vh peptide competitively inhibits the ACh-induced interaction between endogenous vinculin and talin (Fig. 4), inhibits the recruitment of endogenous vinculin to the membrane (Fig. 5), and inhibits vinculin phosphorylation on Tyr-1065 (Fig. 6) in contrast to EGFP-VhA50I, which had no effect. Our observation that the inhibition of

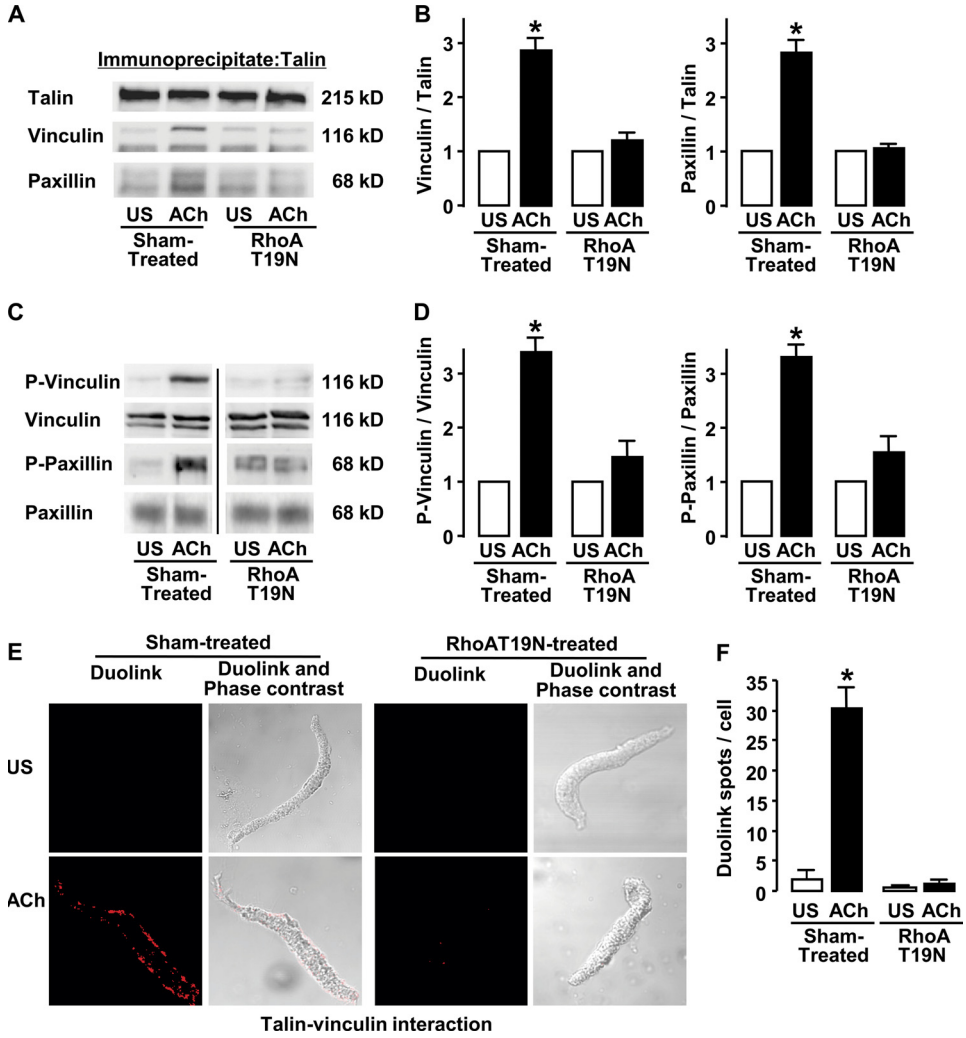

FIGURE 12. **Inactivation of RhoA in tracheal smooth muscle tissues inhibits the ACh-induced increase in the interaction between vinculin and talin and inhibits phosphorylation of vinculin Tyr-1065 and paxillin Tyr-118.** *A*, talin was immunoprecipitated from sham-treated and RhoAT19N-treated tissues stimulated with 10^{-4} M ACh for 5 min or left unstimulated. More vinculin and paxillin co-precipitated with talin in tissues stimulated with ACh in sham-treated tissues, but not in RhoAT19N-treated tissues. *B*, mean ± S.E. relative amounts of vinculin and paxillin that co-precipitated with talin from each treatment group. *, significant difference between ACh-stimulated and US tissues ($n = 3$, $p < 0.05$). *C*, immunoblot of phospho-vinculin (Tyr-1065), total vinculin, phospho-paxillin (Tyr-118), and total paxillin in two sham-treated and two RhoAT19N-treated tissues stimulated with ACh or left unstimulated, respectively. Vinculin and paxillin phosphorylation increased in ACh-stimulated tissues from sham-treated tissues but not in RhoAT19N-treated tissues. *D*, mean ratios of phospho-vinculin over total vinculin and phospho-paxillin over total paxillin from each treatment. In sham-treated tissues, phospho-vinculin and phospho-paxillin in ACh-stimulated tissues were significantly higher than in unstimulated tissues ($n = 5$, $p < 0.05$). In RhoAT19N-treated tissues, phospho-vinculin and phospho-paxillin were not significantly different in US and ACh-stimulated tissues ($n = 5$, $p > 0.05$). *E*, RhoA Inactivation in tracheal smooth muscle tissues inhibited the ACh-stimulated increase in the interaction between talin and endogenous vinculin, as detected by Duolink *in situ* proximity ligation assay on freshly dissociated cells. Each fluorescent spot indicates interaction between talin and endogenous vinculin. *Left panels*, sham-treated cells. *Right panels*, RhoA-inactivated cells. *F*, the total number of Duolink spots was significantly higher in sham-treated ACh-stimulated SMCs (US, $n = 27$; ACh, $n = 34$) than in cells expressing RhoAT19N (US, $n = 30$; ACh, $n = 30$). All of the values are the means ± S.E. *, significantly different from US tissues or cells with the same treatment ($p < 0.05$).

vinculin activation also inhibited the ACh-stimulated phosphorylation of endogenous vinculin at Tyr-1065 suggests that phosphorylation at this site occurs in conjunction with vinculin activation.

We found that the recruitment of vinculin to adhesion complexes and its conversion to an activated state plays an important role in the regulation of active tension development during contraction. Previous studies have suggested a role for vinculin in strengthening the resistive tension of adhesion complexes. Mechanical stress applied to ligand-bound integrins either by stretching or applying force or shear stress to the outside of cells or by actomyosin contraction inside cells results in the enlargement of focal adhesions (19, 20, 22, 52, 53). Using FRET probes, Chen *et al.* (30) demonstrated that vinculin in the activated actin-binding conformation is concentrated in a peripheral band of focal adhesion complexes in spreading cells, whereas vinculin in the cytoplasm is in the autoinhibited conformation. In smooth muscle, the activation of vinculin during contractile stimulation may enable the formation of additional connections between integrin adhesion junctions and cytoskeletal actin filaments and thereby facilitate an increase in the amount of force that can be transmitted across these junctions during active muscle contraction.

We considered the possibility that the membrane recruitment and activation of vinculin in the tracheal tissues

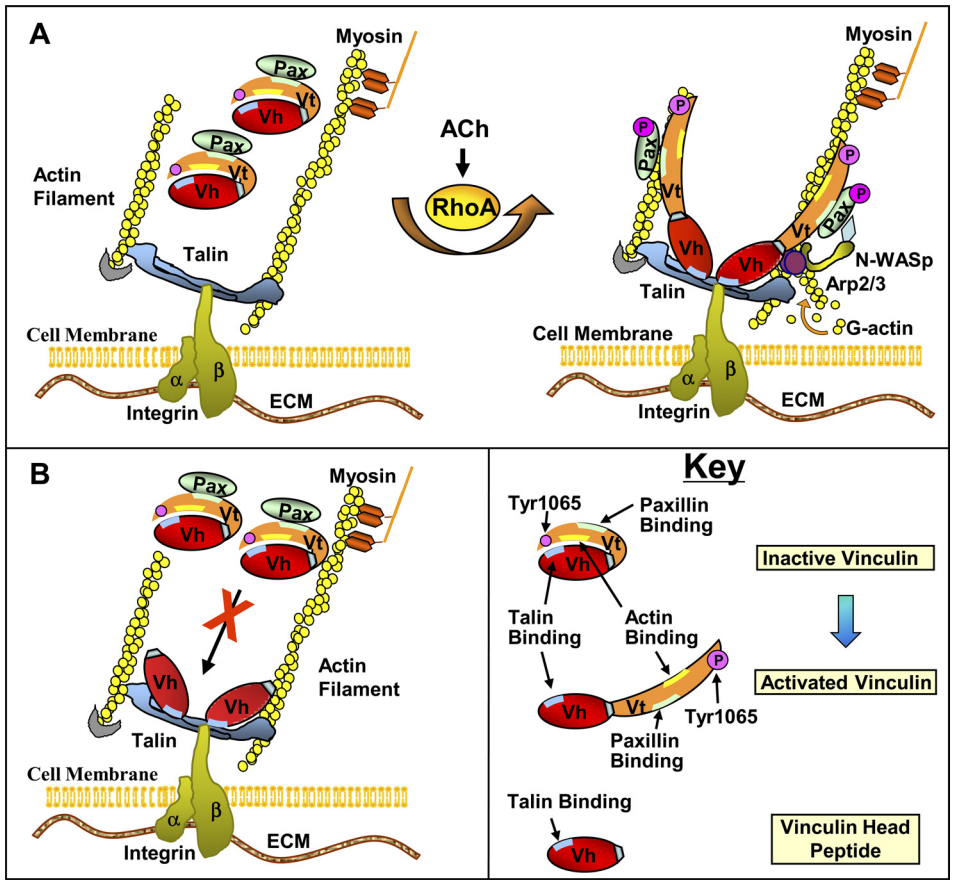

FIGURE 13. **Model for proposed effects of contractile stimulation with ACh on vinculin activity in smooth muscle.** *A*, in unstimulated muscle cells, autoinhibited vinculin in the cytoplasm is bound to paxillin at its tail domain (Vt), but it does not bind to talin or actin filaments at adhesion junctions because the binding sites are obstructed. The vinculin phosphorylation site Tyr-1065 may also be obstructed. Stimulation of the cell with ACh stimulates activation of the small GTPase RhoA and the recruitment of the vinculin-paxillin complex to adhesion junctions, where vinculin interacts with talin on its head domain (Vh) and with other ligands. This catalyzes a conformational change in vinculin to an activated state in which vinculin can bind to F-actin on its tail domain (Vt) and be phosphorylated at Tyr-1065 on its tail domain. The binding of activated vinculin to F-actin and talin strengthens the adhesion junction and enhances the transmission of contractile tension generated by actomyosin cross-bridge cycling. The activated vinculin-paxillin complex also mediates the polymerization of actin by the Arp2/3 complex. *B*, the truncated head domain of vinculin (EGFP-Vh) binds to talin with much higher affinity than autoinhibited endogenous vinculin. EGFP-Vh thus blocks talin binding by endogenous vinculin and inhibits endogenous vinculin activation. However, EGFP-Vh cannot bind to actin or paxillin because their binding sites are located on the tail domain (Vt); thus, it cannot strengthen adhesion junctions or catalyze actin polymerization.

might occur in response to mechanical tension generated by the contractile apparatus or be consequent to the activation of contractile proteins. Muscle tissues were treated with a MLC kinase inhibitor, ML-7, that inhibits MLC phosphorylation and active tension development in response to ACh in canine tracheal smooth muscle tissues (12); however, we observed no effect of ML-7 on the ACh-stimulated interaction of vinculin with talin or on vinculin phosphorylation (Fig. 9). Conversely, the inhibition of vinculin activation had no effect on ACh-induced MLC phosphorylation. This suggests that the vinculin is not activated as a result of tension development by the contractile apparatus and that it is regulated independently from the activation of myosin and cross-bridge cycling. This is consistent with the hypothesis that the recruitment and activation of vinculin at adhesion junctions regulates the ability of the cells to transmit tension generated by the contractile apparatus to the extracellular matrix and that this occurs independently of the activation of cross-bridge cycling.

Our results also suggested that vinculin activation may be a critical step in the initiation of cytoskeletal events that catalyze actin polymerization in response to contractile stimulation of tracheal smooth muscle (Fig. 10). Because actin polymerization is critical for active tension development in tracheal smooth muscle, its suppression would depress active tension generation. Vinculin may directly catalyze the activation of the actin-related protein (Arp)2/3 complex (36), which plays a key role in the process of actin filament polymerization (54). Alternatively vinculin might regulate actin polymerization through its ligand, paxillin. Vinculin and paxillin are both recruited to adhesion sites upon the contractile activation of tracheal SMCs (26), and paxillin undergoes phosphorylation at Tyr-118 and Tyr-31 (3, 4). Paxillin phosphorylation catalyzes the activation of cdc42 and N-WASp via its interactions with the SH2/SH3 adaptor protein, Crk II, leading to activation of the Arp2/3 complex (40, 43, 55). We observed that the expression of EGFP-Vh inhibited the recruitment of both vinculin and paxillin to the membrane and that it also inhibited paxillin phosphorylation on Tyr-

118 (Figs. 5 and 11). By inhibiting the membrane recruitment and phosphorylation of paxillin, the inhibition of vinculin activation by EGFP-Vh may inhibit the signaling pathway that regulates stimulus-induced actin polymerization (Fig. 13).

ACh stimulation of tracheal smooth muscle activates the small GTPase RhoA, which mediates tension generation by regulating stimulus-induced actin polymerization (12). We found that the interaction of vinculin with talin at the smooth muscle membrane and its phosphorylation at Tyr-1065 depend on the activation of RhoA. Thus, RhoA couples the stimulation of muscarinic receptors by ACh to the activation of vinculin.

In tracheal smooth muscle, contractile stimuli initiate the recruitment of multiple cytoskeletal proteins to form a macromolecular complex at membrane adhesion junctions that catalyzes the polymerization of a pool of actin (3, 4). These processes appear to be essential for force development and to be independent of the processes that regulate cross-bridge cycling. The evidence suggests that the pool of actin that undergoes polymerization in response to a contractile stimulus is relatively small and is distinct from the contractile actin that interacts with myosin to activate actomyosin cross-bridge cycling. These findings suggest a model of smooth muscle contraction in which submembranous actin polymerization and the fortification of adhesion junctions support the transmission of force generated by the contractile apparatus to the extracellular matrix (3, 4).

Our results suggest a novel role for vinculin in the regulation of contraction and tension development in smooth muscle (Fig. 13). We found that contractile stimulation actively regulates the cellular localization of vinculin and its activation state, thereby enabling it to interact with the integrin-binding protein talin and with actin. Thus, vinculin activation may facilitate the strengthening and fortification of adhesion junctions that link the contractile apparatus to the extracellular matrix. Furthermore, we found that the activation of vinculin promotes actin polymerization during active tension development. Thus, the regulated activation of vinculin during contractile stimulation appears to be critical for cytoskeletal processes that are essential for the development of active tension in smooth muscle.

Acknowledgments—We are grateful to Dr. Susan Craig (Johns Hopkins University School of Medicine) for generous assistance and donation of vinculin constructs and reagents and for helpful discussions.

REFERENCES

1. Murphy, R. A. (1994) *FASEB J.* **8,** 311–318
2. Murphy, R. A. (1989) *Annu. Rev. Physiol.* **51,** 275–283
3. Gunst, S. J., and Zhang, W. (2008) *Am. J. Physiol. Cell Physiol.* **295,** C576–C587
4. Zhang, W., and Gunst, S. J. (2008) *Proc. Am. Thorac. Soc.* **5,** 32–39
5. Saito, S. Y., Hori, M., Ozaki, H., and Karaki, H. (1996) *J. Smooth Muscle Res.* **32,** 51–60
6. Mehta, D., and Gunst, S. J. (1999) *J. Physiol.* **519,** 829–840
7. Cipolla, M. J., Gokina, N. I., and Osol, G. (2002) *FASEB J.* **16,** 72–76
8. Zhang, W., Wu, Y., Du, L., Tang, D. D., and Gunst, S. J. (2005) *Am. J. Physiol. Cell Physiol.* **288,** C1145–C1160
9. Chen, X., Pavlish, K., Zhang, H. Y., and Benoit, J. N. (2006) *Am. J. Physiol. Heart Circ. Physiol.* **290,** H1915–H1921
10. Rembold, C. M., Tejani, A. D., Ripley, M. L., and Han, S. (2007) *Am. J. Physiol. Cell Physiol.* **293,** C993–C1002
11. Kim, H. R., Gallant, C., Leavis, P. C., Gunst, S. J., and Morgan, K. G. (2008) *Am. J. Physiol. Cell Physiol.* **295,** C768–C778
12. Zhang, W., Du, L., and Gunst, S. J. (2010) *Am. J. Physiol. Cell Physiol.* **299,** C298–C306
13. Johnson, R. P., and Craig, S. W. (1995) *Nature* **373,** 261–264
14. Cohen, D. M., Kutscher, B., Chen, H., Murphy, D. B., and Craig, S. W. (2006) *J. Biol. Chem.* **281,** 16006–16015
15. Bass, M. D., Smith, B. J., Prigent, S. A., and Critchley, D. R. (1999) *Biochem. J.* **341,** 257–263
16. Bois, P. R., Borgon, R. A., Vonrhein, C., and Izard, T. (2005) *Mol. Cell Biol.* **25,** 6112–6122
17. Johnson, R. P., and Craig, S. W. (1994) *J. Biol. Chem.* **269,** 12611–12619
18. Humphries, J. D., Wang, P., Streuli, C., Geiger, B., Humphries, M. J., and Ballestrem, C. (2007) *J. Cell Biol.* **179,** 1043–1057
19. Galbraith, C. G., Yamada, K. M., and Sheetz, M. P. (2002) *J. Cell Biol.* **159,** 695–705
20. Riveline, D., Zamir, E., Balaban, N. Q., Schwarz, U. S., Ishizaki, T., Narumiya, S., Kam, Z., Geiger, B., and Bershadsky, A. D. (2001) *J. Cell Biol.* **153,** 1175–1186
21. DeMali, K. A., and Burridge, K. (2003) *J. Cell Sci.* **116,** 2389–2397
22. Balaban, N. Q., Schwarz, U. S., Riveline, D., Goichberg, P., Tzur, G., Sabanay, I., Mahalu, D., Safran, S., Bershadsky, A., Addadi, L., and Geiger, B. (2001) *Nat. Cell Biol.* **3,** 466–472
23. North, A. J., Galazkiewicz, B., Byers, T. J., Glenney, J. R., Jr., and Small, J. V. (1993) *J. Cell Biol.* **120,** 1159–1167
24. Small, J. V. (1985) *EMBO J.* **4,** 45–49
25. Geiger, B., Dutton, A. H., Tokuyasu, K. T., and Singer, S. J. (1981) *J. Cell Biol.* **91,** 614–628
26. Opazo Saez, A., Zhang, W., Wu, Y., Turner, C. E., Tang, D. D., and Gunst, S. J. (2004) *Am. J. Physiol. Cell Physiol.* **286,** C433–C447
27. Kim, H. R., Hoque, M., and Hai, C. M. (2004) *Am. J. Physiol. Cell Physiol.* **287,** C1375–C1383
28. Bakolitsa, C., Cohen, D. M., Bankston, L. A., Bobkov, A. A., Cadwell, G. W., Jennings, L., Critchley, D. R., Craig, S. W., and Liddington, R. C. (2004) *Nature* **430,** 583–586
29. Chen, H., Choudhury, D. M., and Craig, S. W. (2006) *J. Biol. Chem.* **281,** 40389–40398
30. Chen, H., Cohen, D. M., Choudhury, D. M., Kioka, N., and Craig, S. W. (2005) *J. Cell Biol.* **169,** 459–470
31. Ziegler, W. H., Liddington, R. C., and Critchley, D. R. (2006) *Trends Cell Biol.* **16,** 453–460
32. Cohen, D. M., Chen, H., Johnson, R. P., Choudhury, B., and Craig, S. W. (2005) *J. Biol. Chem.* **280,** 17109–17117
33. Izard, T., Evans, G., Borgon, R. A., Rush, C. L., Bricogne, G., and Bois, P. R. (2004) *Nature* **427,** 171–175
34. Izard, T., and Vonrhein, C. (2004) *J. Biol. Chem.* **279,** 27667–27678
35. Zhang, Z., Izaguirre, G., Lin, S. Y., Lee, H. Y., Schaefer, E., and Haimovich, B. (2004) *Mol. Biol. Cell* **15,** 4234–4247
36. DeMali, K. A., Barlow, C. A., and Burridge, K. (2002) *J. Cell Biol.* **159,** 881–891
37. Turner, C. E., Glenney, J. R., Jr., and Burridge, K. (1990) *J. Cell Biol.* **111,** 1059–1068
38. Turner, C. E. (2000) *Nat. Cell Biol.* **2,** E231–E236
39. Strassheim, D., May, L. G., Varker, K. A., Puhl, H. L., Phelps, S. H., Porter, R. A., Aronstam, R. S., Noti, J. D., and Williams, C. L. (1999) *J. Biol. Chem.* **274,** 18675–18685
40. Tang, D. D., Turner, C. E., and Gunst, S. J. (2003) *J. Physiol.* **553,** 21–35
41. Zhang, W., and Gunst, S. J. (2006) *J. Physiol* **572,** 659–676
42. Söderberg, O., Gullberg, M., Jarvius, M., Ridderstråle, K., Leuchowius, K. J., Jarvius, J., Wester, K., Hydbring, P., Bahram, F., Larsson, L. G., and Landegren, U. (2006) *Nat. Methods* **3,** 995–1000
43. Tang, D. D., Zhang, W., and Gunst, S. J. (2005) *J. Biol. Chem.* **280,** 23380–23389

44. Zhao, R., Du, L., Huang, Y., Wu, Y., and Gunst, S. J. (2008) *J. Biol. Chem.* **283,** 36522–36531
45. Hathaway, D. R., and Haeberle, J. R. (1985) *Am. J. Physiol.* **249,** C345–C351
46. Gilmore, A. P., and Burridge, K. (1996) *Nature* **381,** 531–535
47. Bubeck, P., Pistor, S., Wehland, J., and Jockusch, B. M. (1997) *J. Cell Sci.* **110,** 1361–1371
48. Wang, Z., Pavalko, F. M., and Gunst, S. J. (1996) *Am. J. Physiol.* **271,** C1594–C1602
49. Wood, C. K., Turner, C. E., Jackson, P., and Critchley, D. R. (1994) *J. Cell Sci.* **107,** 709–717
50. Turner, C. E., Kramarcy, N., Sealock, R., and Burridge, K. (1991) *Exp. Cell Res.* **192,** 651–655
51. Bakolitsa, C., de Pereda, J. M., Bagshaw, C. R., Critchley, D. R., and Liddington, R. C. (1999) *Cell* **99,** 603–613
52. Zaidel-Bar, R., Ballestrem, C., Kam, Z., and Geiger, B. (2003) *J. Cell Sci.* **116,** 4605–4613
53. Delanoë-Ayari, H., Al, K. R., Vallade, M., Gulino-Debrac, D., and Riveline, D. (2004) *Proc. Natl. Acad. Sci. U.S.A.* **101,** 2229–2234
54. Pollard, T. D., and Cooper, J. A. (1986) *Annu. Rev. Biochem.* **55,** 987–1035
55. Tang, D. D., and Gunst, S. J. (2004) *J. Biol. Chem.* **279,** 51722–51728